

UDK 546.831; 622.785

## Relation Between Mechanical and Textural Properties of Dense Materials of Tetragonal and Cubic Zirconia

Sofía Gómez<sup>1\*</sup>, Gustavo Suárez<sup>1,2</sup>, Nicolás M. Rendtorff<sup>1,2</sup>, Esteban F. Aglietti<sup>1,2\*</sup>.

<sup>1</sup>Centro de Tecnología de Recursos Minerales y Cerámica (CETMIC CIC-CONICET-CCT La Plata) Argentina.

<sup>2</sup>Departamento de Química, Facultad de Ciencias Exactas - UNLP, Argentina.

Corresponding authors:

---

### Abstract:

*In the current paper we present a study of the sinterability of two zirconia ( $ZrO_2$ ) nanopowders with different content of yttrium oxide ( $Y_2O_3$ ) 3 and 8 % tetragonal and cubic zirconia, respectively. After sintering between 900-1500°C, the samples were characterized in terms of their density and porosity using Archimedes technique. Their grain size was evaluated using scanning electron microscope (SEM). Vickers hardness and fracture toughness ( $K_{IC}$ ) were measured by the indentation method. The results showed that pores are almost eliminated at sintering temperatures higher than 1400°C and grain size is larger due to the agglomerates formed as a result of grain growth. Vickers hardness evaluated at 1400°C sintering temperature is greater than that obtained at 1500°C due to the grain growth produced at this temperature. In addition, we show a correlation between Vickers hardness and the porosity, obtained by evaluating empirical and theoretical models.*

**Keywords:** Zirconia, Sintering, Vickers hardness.

---

## 1. Introduction

Nanocomposites or nanomaterials have at least one of their phases with dimensions of less than 100 nanometers ( $1\text{ nm} = 10^{-9}\text{ m}$ ). Decades of research have shown that the degree of homogeneity of particle packing in the green body has an enormous impact on sintering characteristic. In this regard, nanocrystalline powders are at a severe disadvantage due to the effects of agglomeration. In most dry nanocrystalline powders the crystallites are strongly bonded together to form agglomerates. This leads to both intra-agglomerate and inter-agglomerate porosity, the former generally being at the nanoscale whilst the latter is at the submicron or even micron level, particularly if the powders suffer from multiple levels of agglomeration [1-2].

Nanostructured materials appear seem to be an appropriate alternative to overcome the microstructured and monolithic limitations. Their outstanding properties make them attractive to be studied [3]. For example, Vickers hardness tests have suggested that nanocrystalline ceramics are softer than large grained ceramics at room temperature and so tend to crack less [4-6].

Moreover, a number of studies have determined that various properties of consolidated solids are a function of the total porosity independently of consolidation or sintering [7-8]. For instance, Cho et al. have adjusted the interdependence between Hv and

---

\*) **Corresponding author:** sofia.gomez@cetmic.unlp.edu.ar; eaglietti@cetmic.unlp.edu.ar

porosity in alumina system with regular mathematical model. Furthermore Zivcová et al. have studied theoretical models which relate Young's module and the porosity.

However, little is known about a particular model representing a relationship between Vickers hardness and porosity. We show a correlation between Vickers hardness and the porosity, obtained by evaluating empirical and theoretical models.

In this paper we present a study of sinterability from samples consolidated by uniaxial pressing and we propose the characterization of a series of zirconia ( $ZrO_2$ ) nanopowders with different content of yttrium oxide ( $Y_2O_3$ ) 3 and 8 % mol ( $D_{50} \leq 100nm$ ) tetragonal and cubic zirconia, respectively. There are others non-conventional methodologies for sintering ceramics like spark plasma sintering (SPS) and microwave sintering (MW) designed for minimizing the grain growth [9]. However in this work we use conventional sintering to compare the sinterability and properties of 3Y and 8Y zirconia. We used zirconia because it is a versatile ceramic material with excellent mechanical properties and many applications ranging from refractories to biomaterials and fuel cells [10-11].

## 2. Experimental procedures

Two commercial powders of zirconia (Tosoh Corporation, Tokyo, Japan) were used. Tab. I shows the material characteristics. Characterization of starting powders included evaluation of the size and grain morphology by scanning electron microscopy (SEM). To obtain a better observation, samples were metalized with gold. Crystallinity of powders was evaluated by X-ray diffraction (XRD) and the structure was also examined by Rietveld refinement method.

**Tab. I.** Characteristics of the zirconia nanopowders.

Properties	TZ-3Y	TZ-8Y
Content of $Y_2O_3$ (mol%)	3	8
Specific Area ( $m^2/g$ )	16±3	12.7
Theoretical Density ( $g/cm^3$ )	6.05	5.90
Denomination	3Y	8Y
Average equivalent Diameter (nm)*	62.0	80.1

\*Average equivalent diameter was calculated using theoretical density and specific area considering spherical particles shape.

Zirconia nanopowders ( $ZrO_2$ ) with different content of yttrium oxide ( $Y_2O_3$ ) were uniaxially pressed in 15 mm diameter samples, the pressure applied was  $500 kg/cm^2$  and 0.5 % of polyvinyl alcohol (PVA) was used as binder. Samples were sintered on an electric furnace with identical heating and cooling velocity and permanence,  $5^\circ C/min$  and 180 minutes, respectively. After sintering, samples were characterized in terms of their density and porosity using Archimedes technique. Their grain size was evaluated using a scanning electron microscope (SEM). Average diameter was indirectly measured by quantification of grains in SEM images. Values were obtained from calculation of each grain area using a circumference area as a model of grain.

Vickers hardness was measured by the indentation method at loads of 0.5 kg applied for 15 seconds. The fracture toughness ( $K_{IC}$ ) was calculated by the indentation method from the evaluation of the cracks that develop in the vertices of the imprint Vickers [4].  $K_{IC}$  was defined as shown in the following expression:

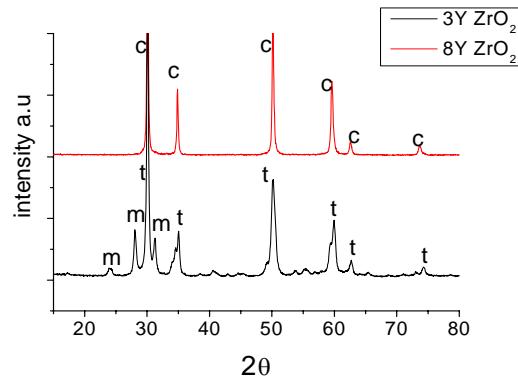
$$K_{IC} = \delta \left( \frac{E}{Hv} \right)^{0.5} \cdot \frac{P}{c^{\frac{3}{2}}} \quad (1)$$

Where E is the elastic modulus (210 GPa for zirconia [7]), Hv is the Vickers Hardness, P is the indentation test load in Newton, c is the indentation crack length and  $\delta$  is a constant (0.018) [12]. Finally, the thermal treatment effect over crystalline phases was determined by XRD ( $2\theta$  between  $5^\circ$  y  $80^\circ$ , 0,04 for step and time of 2 seconds).

### 3. Results and discussion

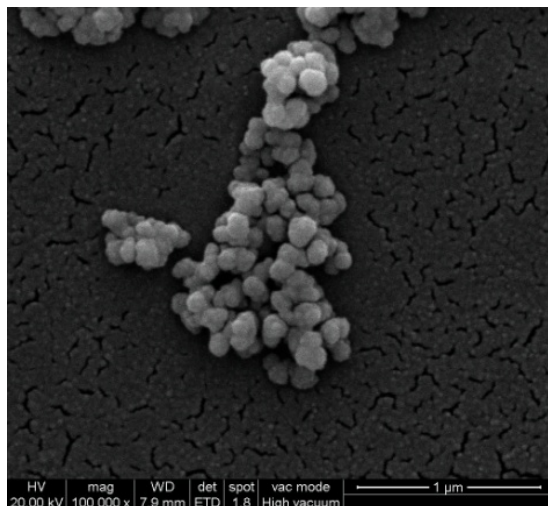
#### Starting powders characterization

Fig. 1 shows the two starting powders diffraction patterns. Clearly, phases present in powders are as follows: partially stabilized zirconia powder (3Y) presents tetragonal zirconia as the main phase (67,3%) and small peaks corresponding to the monoclinic phase (32,7%). The quantification was determined by the Rietveld refinement method [13-14]. Fully stabilized zirconia powder (8Y) presents peaks corresponding to the cubic phase.



**Fig. 1.** Diffraction patterns of the commercial powders: 3Y-ZrO<sub>2</sub> and 8Y-ZrO<sub>2</sub>.

Fig. 2 shows SEM micrograph of 3Y powder. Sample preparation consisted of fast dispersion of powders in water and posterior evaporation on a glass. This commercial nanopowder tends to agglomerate. It presents rounded morphology and bounded granulometric distribution of approximately 100 nm.



**Fig. 2.** SEM micrograph of 3Y powder.

Fig. 3 shows a SEM micrograph of

8Y powder, which presents similar characteristics, such as rounded morphology and the tendency to agglomerate. Grain size in the order of 100 nm is also observed.

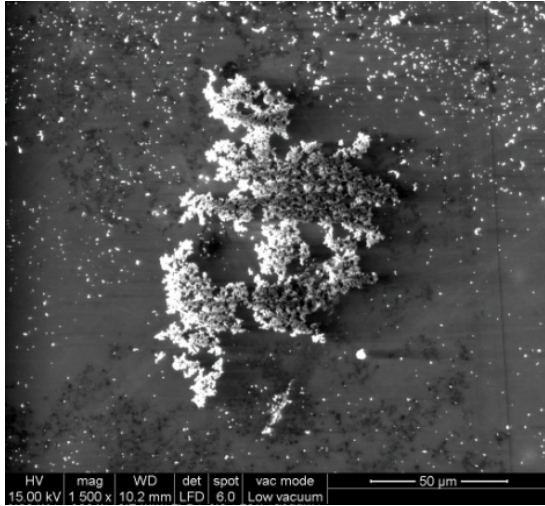


**Fig. 3.** SEM micrograph of 8Y powder.

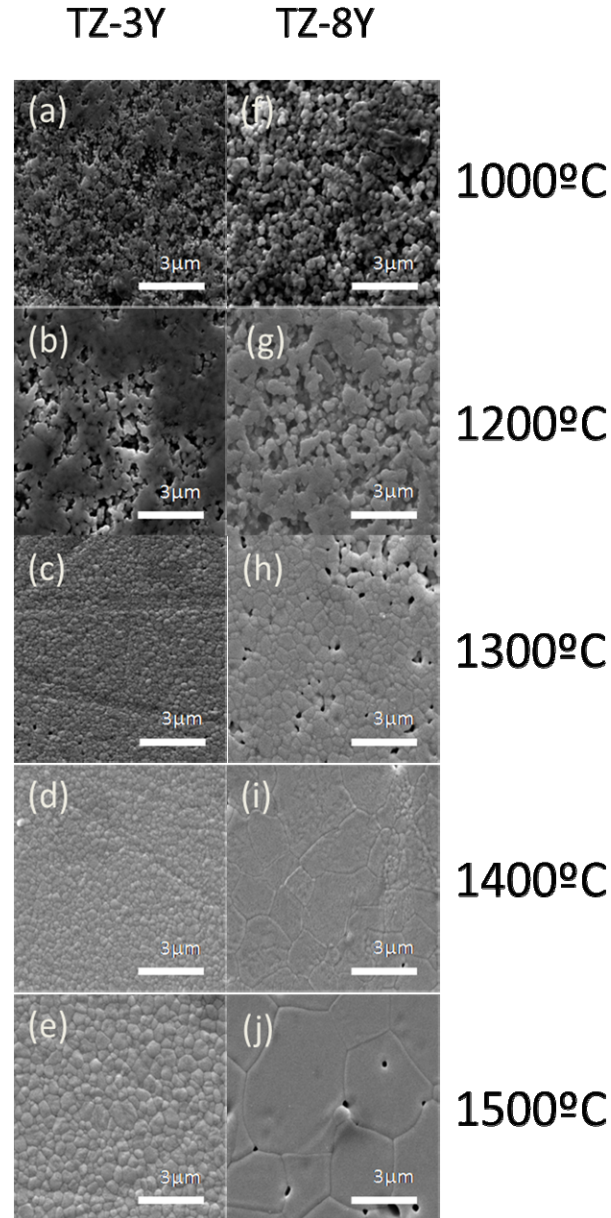
### 3.1. Textural properties (sinterability)

Fig. 4 shows SEM micrographs of 1000, 1200, 1300, 1400 and 1500°C tetragonal and cubic materials. It is observed that in general, porosity decreases and density increases with increasing temperature (Figs 6 a) and b)). Materials based on tetragonal and cubic zirconia sintered at 1000°C show a significant porosity. Figs 4 a) and f) clearly present the incomplete sintering.

At 1200°C grains appear bound forming a developed neck between them (Fig. 4 b) and g)). Furthermore, some pores (in black) had been detected by Archimedes method. The material is partially densified. Figs 4 c) and h) show the materials at 1300°C. In this case the sintering is complete, but porosity is still greater than zero. This is more noticeable for cubic zirconia material (Fig. 4 h)), wherein the porosity is about 10%. Finally, at a sintering temperature of 1400°C the material presents a noticeable homogeneity. This fact indicated that the sintering conditions employed were enough to reach the complete sintering. By the time that the latter porosity has been eliminated by sintering, grain growth can cause the individual nanoparticles to sinter together yielding a final grain size approximating to that of original agglomerates [2]. Thus, at sintering temperatures higher than 1300°C grain size increment rapidly for the cubic zirconia reaching at 1500°C a grain size up to 4,5 μm (Fig. 4 j)).

Fig. 5 shows that the average diameter suffers a small increase ranging from 100 nm (starting powders) to 300 nm approximately for both 3Y and 8Y during the formation of developed neck until the complete sintering of the material at 1300°C. As from 1300°C two situations can be appreciated: on one hand the 3Y average diameter remains constant (approximately 500 nm); on the other hand the average diameter increases markedly with the sintering temperature for 8Y (0,5 μm to 4,5 μm) affecting hardness, as will be seen below. The comparison between the starting powder diameter and the sintered grain size shows that in both cases (3Y and 8Y) the diameter is less than 100 nm (Tab. 1) while the grain size for all the complete sintered materials is greater than 400 nm. This demonstrates the tendency of nanomaterials to form very resistant agglomerates due to the processing route. The high mobility of the oxygen ions yttria stabilizing zirconia together with the high melting point suggests that the cation diffusion will be controlling the diffusion in these materials. 8Y normally has a faster grain growth than that in tetragonal zirconia [15]. It was observed that 8Y presents a higher diffusion coefficient ( $6.00 \times 10^{-11}$ ) than that for 3Y ( $4.05 \times 10^{-14}$ ) [11].

These values support the idea of a faster sintering and grain growth for 8Y. This is in agreement with Fig. 5 and it could even be observed in the increase of grain size with temperature in Fig. 4.

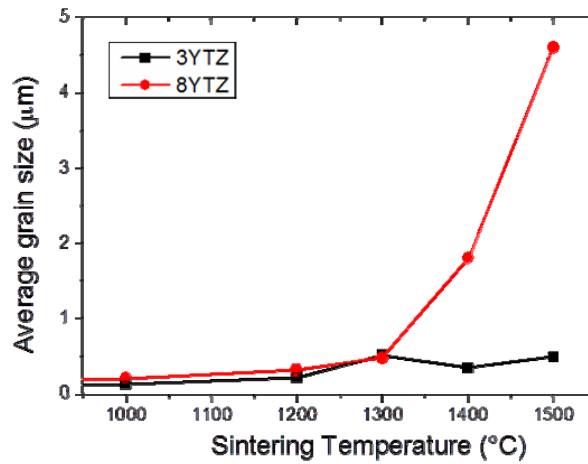


**Fig. 4.** SEM micrographs of (a-e) tetragonal zirconia at 1000, 1200, 1300, 1400 and 1500°C; (f-j) cubic zirconia at 1000, 1200, 1300, 1400 and 1500°C.

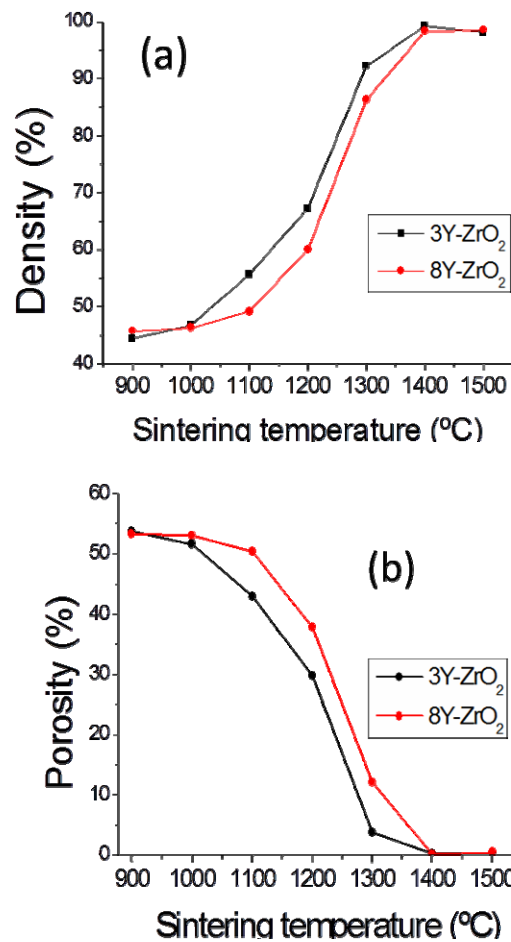
Fig. 6 a) shows the advance of zirconia commercial nanopowders density with the sintering temperatures. It is observed that the two zirconia start from densities of about 45% ( $3 \text{ g/cm}^3$ ) of theoretical corresponding to the densities obtained by the selected route. The sigmoid shape of the densification curves can be observed. They increase progressively with the temperature until finding an asymptotic value at high temperatures. The final densities obtained were 99% for 3Y and 98% for 8Y of their respective theoretical densities, representing an adequate densification despite the simple selected route of manufacture.

Fig. 6 b) shows the porosity thermal evolution. As expected, the porosity behavior is complementary to the Fig. 6 a). The relative porosity of the starting materials is about 50%.

Like density, started porosity was affected by the processing route. As mentioned in the literature review, the processing route (slip casting) allows obtaining a green porosity of approximately 60 % [11-16]. After treatments at 1400 °C the porosity gradually decreases reaching null values for the stabilized zirconia (3Y and 8Y).



**Fig. 5.** Grain average diameter as a function of the sintering temperature.



**Fig. 6.** (a) Density evolution as a function of the sintering temperature. (b) Porosity evolution as a function of the sintering temperature.

As expected, the final density of these samples is 98 or 99 %, and the porosity is null at temperatures above 1400°C. Therefore, there exists a kind of porosity that the Archimedes method cannot evaluate, because this technique only evaluates open porosity.

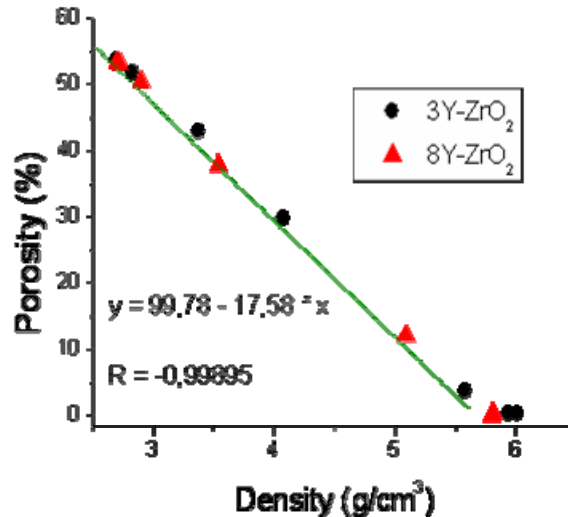


Fig. 7. Correlation between porosity and density for commercial nanopowders.

Fig. 7 shows that both sintering parameters (density and porosity) are directly related regardless the starting powder. This Fig. shows the correlation between porosity and density for all the elaborated materials and the result of a simple lineal fitting.

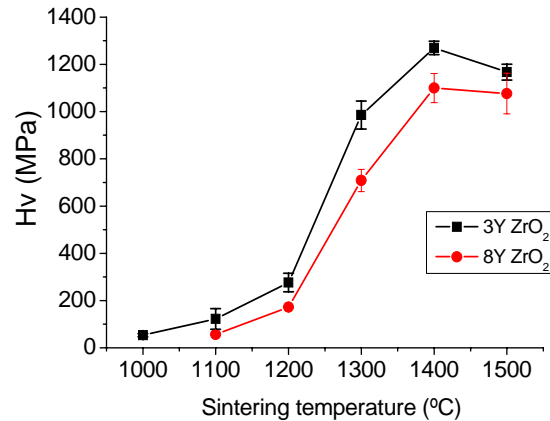
### 3.2. Vickers hardness (Hv)

Fig. 8 shows the values of the Vickers hardness as a function of the sintering temperature for 3Y and 8Y materials. The measured Vickers hardness in our study is in agreement with that described in literature [10]. Partially stabilized zirconia hardness was higher than fully stabilized zirconia hardness throughout the range of temperatures. The sigmoid shape of the curves for both materials can be observed. The maximum values for both starting powders were obtained after treatments at 1400°C.

In Fig. 8 Hv evaluated at 1400°C sintering temperature is greater than that obtained at 1500°C. It is known that sintering causes the formation of solid bonds between particles when they are heated. The bonds reduce the surface energy by removing the free surface; this is followed by a secondary stage of grain growth due to grain boundary elimination [1]. Moreover,

Tab. II. Relation among sintering temperature, grain size, Hv and density.

	T (°C)	Grain size (nm)	Hv (MPa)	Density (g/cm <sup>3</sup> )
3Y-TZ	1300	515	985,5455	5,58
	1400	342	1270,08	6,01
	1500	490	1167,4	5,94
8Y-TZ	1300	475	708,37	5,09
	1400	1801	1099,98	5,8
	1500	4603	1076,66	5,81



**Fig. 8.** Vickers hardness as a function of the sintering temperature.

XRD analysis of 3Y was carried out in order to establish the presence of crystalline composition changes, which remained constant in the studied temperature range. No important changes were observed or cubic phase detected. Therefore, slight Hv decrease observed between 1400 and 1500°C can be attributed to effects of grain size increment rather than to crystalline composition. Figs. 4 e) and j) show that the grain size of 1500°C materials is larger than that of 1400°C materials. Thus, Vickers hardness decreases at 1500°C due to grain growth produced at this temperature. Tab. II shows that the Vickers Hardness decreases as the grain size increases.

### 3.3. Fracture toughness ( $K_{IC}$ )

Fig. 9 shows the values of fracture toughness ( $K_{IC}$ ) of the partially and fully stabilized zirconia as a function of the sintering temperature with its respective errors. It was not possible to measure the fracture toughness for the material constituted by 8Y at 1300°C due to the fact that cracks did not develop well after indentation.

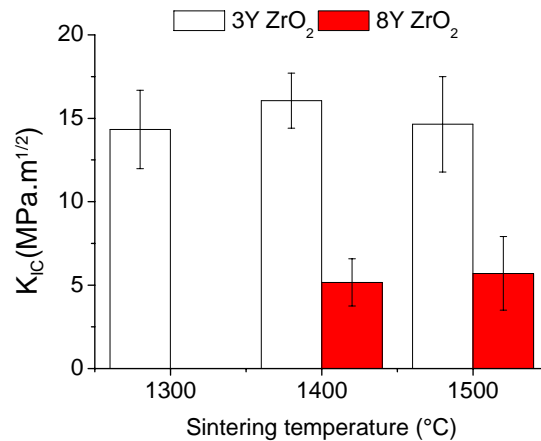


**Fig. 9.** Fracture toughness a function of the sintering temperature.

As expected, the fracture toughness of 3Y materials is notably higher (around 15 MPa.m<sup>1/2</sup>) than that of 8Y materials (5 MPa.m<sup>1/2</sup>). Moreover, the value of  $K_{IC}$  remains relatively constant in the temperature range studied. The measured error in 3Y materials is lower than that in 8Y materials. The values obtained are in agreement with the literature [2] values.



### 3.3. Correlations of Vickers hardness with sintering parameters

The effect of the porosity on the physical properties has been a matter of interest over the past decades. Several properties of sintering solids were determined as a function of porosity regardless the sintering process [7-8].

**Tab. II.** Theoretical models of Vickers hardness.

Model			
1	$Hv = Hv_0(1 - \phi)$		
2	$Hv = Hv_0 \left( \frac{1 - \phi}{1 + \phi} \right)$		
3	$Hv = Hv_0(1 - 2\phi)$		
4	$Hv = Hv_0(1 - \phi)^2$		
5	$Hv = Hv_0 \exp\left(\frac{-2\phi}{1 - \phi}\right)$		
6	$Hv = Hv_0 \left[ \frac{(1 - \phi)^2}{1 + \phi} \right]$		
Exponential (Our work)	$Hv = Hv_0 \exp(-b \cdot \phi)^b$	Hv <sub>0</sub> = 1320,3	b= 4,81

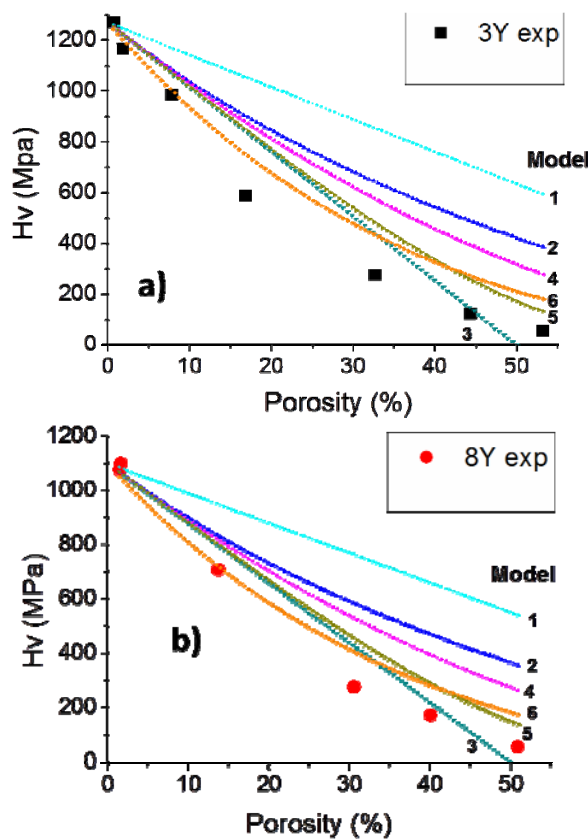


**Fig. 10.** Theoretical predictions for materials a) 3Y and b) 8Y.

Vickers hardness was studied as a function of porosity and the results were compared with theoretical predictions. Six theoretical models were considered to adjust the values of this property. The models are shown in Tab. III, where  $H_v$  is Vickers hardness,  $H_{v0}$  is Vickers hardness at the lowest porosity,  $\Phi$  is porosity and  $b$  is a constant. Furthermore, an exponential adjust using the empiric values of Vickers hardness was obtained. This prediction is also shown in Tab. III. The values of  $H_{v0}$  and  $b$  in the exponential adjust were obtained using least-squares estimation. Moreover,  $b$  resulted near 5, this value agrees with the results of studies by Rice [17] for polyhedral pore shape (tetrahedral and/or octahedral). This morphology is common for pores caused by the imperfect packing of zirconia particles [17-18].

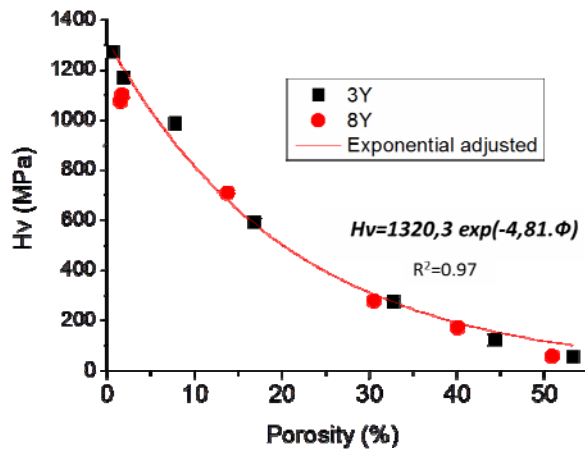


Fig. 11. Exponential adjust of Vickers hardness as a function of porosity.

Figs 10 a) and b) show the theoretical predictions for materials 3Y and 8Y, respectively. It can be observed that porosity under 12% could be represented by model 6 but out of this range, the model overestimated the hardness. Moreover, the exponential adjust constitutes an appropriate expression to represent this relationship regardless the yttrium content (Fig. 11).

#### 4. Conclusions

Characterization of zirconia nanopowders with different content of yttrium ( $Y_2O_3$ ) (3 and 8%) was conducted. These commercial nanopowders tend to agglomerate. They presented rounded morphology and bounded granulometric distribution of approximately 100 nm. The sinterability characterization of the materials and the evolution of textural properties (porosity and density) as a function of temperature were evaluated in the range 900-1500°C. Grain growth can cause the individual nanoparticules to sinter together yielding a final grain size approximating to that of original agglomerates (for cubic material sintering at 1500°C there are grains with sizes up to 1  $\mu$ m).

Mechanical properties (Vickers hardness and fracture toughness) measured were in agreement with those found in the literature. Vickers hardness evaluated at 1400°C sintering temperature is greater than that obtained at 1500°C due to grain growth produced at this temperature. Fracture toughness of 3Y materials is notably higher (around 15  $MPa \cdot m^{1/2}$ ) than that of 8Y materials (5  $MPa \cdot m^{1/2}$ ).

Furthermore, Vickers hardness was studied as a function of porosity and the results were compared with theoretical predictions, showing an exponential correlation between

Vickers hardness and porosity that represent this relationship regardless the yttrium content.

## 5. References

1. G. Suárez, Y. Sakka, T.S. Suzuki, T. Uchikoshi, X. Zhu, E.F. Aglietti, "Effect of starting powders on the sintering of nanostructured ZrO<sub>2</sub> ceramics by colloidal processing", *Science and Technology of Advanced Materials*, 10 (2009) 025004.
2. H.T. Kim, Y.H. Han, "Sintering of nanocrystalline BaTiO<sub>3</sub>", *Ceramics International*, 30 (2004) 1719-1723.
3. Niihara, Koichi, "New design concept of structural ceramics. Ceramic nanocomposites", *Journal of the Ceramic Society of Japan*, 99 (1991), 974-982.
4. J. Binner, B. Vaidyanathan, "Processing of bulk nanostructured ceramics", *Journal of the European Ceramic Society*, 28 (2008) 1329-1339.
5. J. Karch, R. Birringer, H. Gleiter, "Ceramics ductile at low temperature", *Nature*, 330 (1987) 556-558.
6. M.J. Mayo, R.W. Siegel, A. Narayanasamy, W.D. Nix, "Mechanical properties of nanophase TiO<sub>2</sub> as determined by nanoindentation", *Journal of Materials Research*, 5 (1990) 1073-1082.
7. Z. Živcová, M. Černý, W. Pabst, E. Gregorová, "Elastic properties of porous oxide ceramics prepared using starch as a pore-forming agent", *Journal of the European Ceramic Society*, 29 (2009) 2765-2771.
8. S.A. Cho, F.J. Arenas, I. de Arenas, J. Ochoa, J.L. Ochoa, "Porosity; microhardness correlation of sintered (Al<sub>1-y</sub>Cry)<sub>2</sub>O<sub>3</sub> solid solutions", *Rev. LatinAm. Metal. Mater.* 17 (1997) 30-35.
9. K. Rajeswari, U. S. Hareesh, R. Subasri, Dibyendu Chakravarty, R. Johnson "Comparative evaluation of spark plasma (SPS), microwave (MWS), two stage sintering (TSS) and conventional sintering (CRH) on the densification and micro structural evolution of fully stabilized zirconia ceramics", *Science of Sintering*, 42 (2010) 259-267.
10. H.H. Zender, H. Leistner, H.R. Searle, "ZrO<sub>2</sub> materials for application in the ceramic industry", *Interceramics*, 39 (1990) 33-35.
11. G. Suárez, N.M. Rendtorff, A.N. Scian, E.F. Aglietti, "Isothermal sintering kinetic of 3YTZ and 8YSZ: Cation diffusion", *Ceramics International*, 39 (2013) 261-268.
12. K. Niihara, R. Morena, D.P.H. Hasselman, "Evaluation of K<sub>Ic</sub> of brittle solids by the indentation method with low crack-to-indent ratios", *Journal of Materials Science Letters*, 1 (1982) 13-16.
13. H.M. Rietveld, "A profile refinement method for nuclear and magnetic structures", *J. Appl. Crystallogr.*, 2 (1969) 65-71.
14. J. Rodriguez-Carvajal, "FULLPROF: A Program for Rietveld Refinement and Pattern Matching Analysis", *Abstracts of the Satellite Meeting on Powder Diffraction of the XV Congress of the IUCr*, 1990, p. 127-128.
15. R. Chaim, "Activation energy and grain growth in nanocrystalline Y-TZP ceramics", *Materials Science and Engineering A*, 486 (2008) 439-446.
16. G. Suárez, B.K. Jang, E.F. Aglietti, Y. Sakka, "Fabrication of dense ZrO<sub>2</sub>/CNT composites: Influence of bead-milling treatment", *Metallurgical and Materials Transactions A: Physical Metallurgy and Materials Science*, 44 (2013) 4374-4381.

- 
- 17.N. M. Rendtorff, L. B Garrido, E. F. Aglietti, "Porosidad y módulo de elasticidad de cerámicos porosos obtenidos a partir de t-ZrO<sub>2</sub> y almidón , in "IBEROMET IX-X sam/conamet", (2010).
- 18.R.W. Rice. Marcel Dekker, "Porosity of Ceramics: Properties and Applications " New York. (1998).

---

**Садржај:** У овом раду представљена је студија о синтерабилности два цирконијум-оксидна (ZrO<sub>2</sub>) нано праха са различитим уделима итријум оксида (Y<sub>2</sub>O<sub>3</sub>) 3 и 8 % тетрагоналног и кубног цирконијума, истим редоследом. Након синтеровања између 900-1500°C, Архимедесовом техником су одређене густина и порозност. Величина зрна је окарактерисана скенирајућом електронском микроскопијом (SEM). Викерсова тврдоћа и отпорност на лом (K<sub>1C</sub>) мерени су методом индентације. Резултати указују на то да су пре готово елиминисане на температурама синтеровања преко 1400°C и раст зрна је већи услед појаве агломерата. Викерсова чврстоћа на 1400°C синтеровања је већа од оне постигнуте на 1500°C управо због већег раста зрна на вишим температурама. Коначно, указали смо на корелацију између Викерсове чврстоће и порозности, употребом емпиријског и теоријског модела.

**Кључне речи:** цирконијум, синтеровање, Викерсова чврстоћа.

---